

RESEARCH

Open Access



An Adaptive Crack Width Prediction for Flexural Steel Reinforced UHPC Beams

Yanping Zhu^{1,2}, Yang Zhang^{1*}, Xinzhe Yuan² and Changgui Hou¹

Abstract

The crack pattern of steel reinforced ultrahigh performance concrete (UHPC) beam is usually characterized by many densely distributed fine cracks (i.e., multiple microcracks) along with localized macrocrack, and the crack width development rate along the beam height is smaller than that of normal concrete since steel fibers and steel reinforcement bars are supposed to be effective in controlling crack width propagation of the UHPC beam. However, an effective crack width prediction formula is still underdeveloped for steel reinforced UHPC beam. The present study aims to formulate a crack width prediction equation based on the equations in Chinese code GB50010 where the parameters can be regressed and calibrated. Ten UHPC beams with different steel fiber volumes and reinforcing ratios are experimentally tested to collect crack width and spacing data for comparison and validation purposes. Nonuniformity distribution coefficient of rebar strain and average crack spacing are calibrated by the test data. Also, rebar stress is calculated with considering residual tensile strength of UHPC based on a sectional analysis. The modified crack width equation is validated with the test results, showing the best prediction accuracy of 0.97 and standard deviation of 0.11 for the test beams in this study compared to those predicted by JTG 3362, CECS 38, MC and AFGC. This study is emphasizing crack width prediction and control in designing UHPC structures.

Keywords UHPC beams, Crack width, Modification and prediction, Flexural behavior

1 Introduction

Ultrahigh performance concrete (UHPC), one of the most advanced cementitious composite materials, has attracted much attention from structural engineering community and it shows large application potential due to unique mechanical performance (such as multiple cracking behavior and strain hardening capacity) (De Larrard & Sedran, 1994; Graybeal, 2006; Graybeal & Baby, 2013; Meng & Khayat, 2016, 2018; Qiu et al., 2022; Richard & Cheyrezy, 1994; Wille et al., 2014; Yoo

et al., 2016a). In the past 15 years, the research on UHPC has grown exponentially as shown in Fig. 1 and the use of UHPC for infrastructure construction is becoming increasingly popular. Many studies focus on mechanical behavior of UHPC structures under different loads and environment conditions in order for their design and use (Brühwiler, 2017; Feng et al., 2021; Habel et al., 2007; Hussein et al., 2022; Zhou et al., 2022; Zhu et al., 2020, 2022). Concrete cracking is an important issue for concrete structures historically (Borosnyoi & Balazs, 2005; Hong et al., 2013; Piyasena et al., 2004). Generally, the crack pattern (or failure mode) and crack propagation of UHPC members under flexure or tension have been well recorded and described in the following studies.

Yoo et al. (2017) investigated flexural behavior of UHPC beams with low reinforcement ratios and concluded that numerous vertical micro-cracks appeared near the peak load and then the crack localization happened with decreasing carrying-load capacity. The

Journal information: ISSN 1976-0485 / eISSN 2234-1315.

*Correspondence:

Yang Zhang
zhangbridge@hnu.edu.cn

¹ College of Civil Engineering, Hunan University, Changsha 410082, Hunan, China

² Civil, Architectural and Environmental Engineering, Missouri University of Science and Technology, Rolla, MO 65401, USA

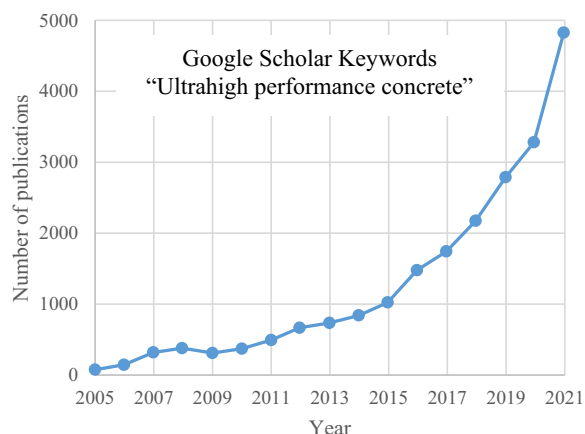


Fig. 1 Number of publications on UHPC from an investigation by HIPER FIBER LLC



Fig. 2 Example of multiple cracking and localized crack in this study

reinforcement ratio marginally influenced the number of cracks and average crack spacing. Yang et al. (2010) found that the tightly spaced cracks on the lower surface of the beam perpendicular to flexural tensile stress were associated with stress redistribution and multiple cracking, which was different from the development pattern of flexural cracks in normal concrete beams. The fiber bridging capacity and pullout at the highly stressed crack dominated the flexural failure and the steel fibers were effective in controlling cracks. The multiple microcracks and localized macro-cracks in the rebar reinforced UHPC beams were also observed by Chen et al. (2018), Qi et al. (2018), and Hasgul et al. (2018). With increasing reinforcement ratio and using hybrid reinforcement, the number of cracks decreased and the average crack spacing increased, controlling the crack width of reinforced UHPC beams (Yoo et al., 2016b). One example of multiple cracking and localized crack is shown in Fig. 2 in this study.

The entire crack patterns and developments of UHPC are well reported, but the maximum crack width predictions associated with crack spacing and rebar stress are not fully studied, although relatively mature crack width predictions for normal concrete have been developed experimentally, analytically, and numerically. Leutbecher and Fehling (2012) proposed a mechanics-based model

to predict the crack formation process (i.e., crack spacing and width) of the UHPC with reinforcing bars and fibers. The predicted cracking spacing was close to the transverse reinforcing bar spacing for an example of thin, orthogonally reinforced UHPC topping layer applied on an existing concrete structure for rehabilitation purpose. Qiu et al., (2020a, 2020b) experimentally investigated flexural cracking behavior of eight UHPC beams with different reinforcement ratios, reinforcement diameters and cover thicknesses. Their crack patterns, crack spacings, and load-crack width curves were compared. Also, the crack widths of UHPC beams were predicted by existing codes, such as CECS (2004), NF-P18-710 (2016), CNR-DT (2006), MC (CEB-FIP 2010) and RILEM 162-TDF (2003). Although NF-P18-710 model shows relatively high accuracy, 60% and 25% deviations of predicted and tested mean crack spacing, and maximum crack width were obtainable respectively. Therefore, there are obvious shortcomings and limitations simply using the current crack width prediction theory for UHPC beam and the new UHPC crack width prediction is still underdeveloped. The present study is an attempt to develop a modified crack width prediction for steel reinforced UHPC beams in accordance with Chinese code GB (2010). The crack width data were experimentally collected through testing ten UHPC beams with different steel reinforcement ratios and fiber volumes. Different existing codes for predicting crack width were reviewed and their predicted results were compared to highlight the modification need for crack width prediction of UHPC. Finally, the modified equations were proposed, and some parameters (such as nonuniformity distribution coefficient of rebar strain and average crack spacing) can be calibrated from the test data along with re-consideration of rebar stress through a sectional analysis. The adequacy of the modified equations for crack width prediction was assessed and validated using the data in the present study and other studies.

2 Experimental Investigations

An experimental program was performed to investigate crack widths of five steel reinforced UHPC beams, and each group had two same specimens. The main test variables were the steel fiber volume and reinforcing ratio and the test details are shown in Table 1.

2.1 Material Properties

The UHPC is composed of Portland cement (771.2 kg/m³), silica fume (154.2 kg/m³), fly ash (77.1 kg/m³), quartz powder (154.2 kg/m³), quartz sand (848.4 kg/m³), superplasticizer (20.1 kg/m³), water (180.5 kg/m³), and steel fibers. End-hooked steel fiber with a length of 13 mm and a diameter of 0.2 mm and straight steel fiber

Table 1 Parameters of test specimens

Beam designation	Longitudinal rebar diameter (mm)	Reinforcing ratio (%)	Number of longitudinal rebars	Steel fiber fraction by volume
L2.33%-1.5%-1/2	20	2.33	3	1.5% hooked end
L2.33%-2.0%-1/2	20	2.33	3	2.0% hooked end
L2.33%-3.0%-1/2	20	2.33	3	2.0% hooked end + 1.0% straight
L1.48%-2.0%-1/2	16	1.48	3	2.0% hooked end
L2.83%-2.0%-1/2	22	2.83	3	2.0% hooked end

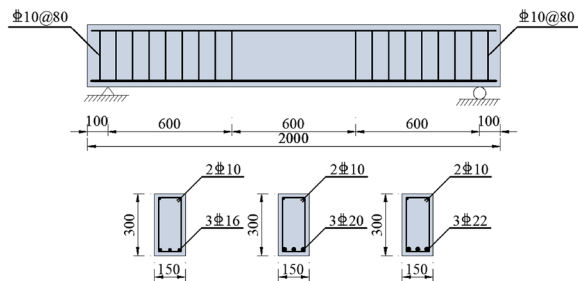


Fig. 3 Specimen details

with a length of 8 mm and a diameter of 0.12 mm were used. Three volume fractions of steel fibers were considered: 1.5% end-hooked fiber; 2% end-hooked fiber; 2% end-hooked fiber + 1% straight fiber. The tensile strength of these steel fibers was greater than 2000 MPa. The cubic compressive strengths of UHPC with fiber volume fractions of 1.5%, 2.0%, and 3.0% are 159 MPa, 167 MPa, and 183 MPa, respectively; the elastic moduli are 47 GPa, 48 GPa, and 49 GPa, respectively; the modified first flexural crack strengths are 7.26 MPa, 7.85 MPa, and 9.05 MPa, respectively. The yield strengths of steel rebar with diameters of 16 mm, 20 mm, and 22 mm are 480 MPa, 495 MPa, and 502 MPa, respectively in this study.

2.2 Specimen Preparation

As shown in Fig. 3, ten UHPC beams were reinforced with three longitudinal rebars and two rebars (diameter of 10 mm) in the tension and compression zones respectively. Three kinds of diameters (i.e., 16 mm, 20 mm, and 22 mm) were considered for the longitudinal tensile rebars. Each measured 300 × 150 mm in cross section and 2000 mm in length along with concrete cover thickness of 20 mm. Steel stirrups (diameter of 10 mm) were arranged at a spacing of 80 mm at the shear-flexure segment of the beam.

The UHPC was sufficiently mixed, and no vibration was needed because of self-compacting capability when casting the beams from one end to the other. After three days, the beams were demolded and subjected to steam

curing at 90–100 °C for two days. Another one day was required for cooling down, and the beams were stored at the laboratory environment until the test.

2.3 Bending Tests

Four-point bending test was performed to investigate flexural cracking characteristics of all the beams and they were loaded by a hydraulic jack to the failure along with the simply supported span of 1800 mm and the pure bending moment length of 600 mm. The load interval was 5 kN until UHPC cracking and became 10 kN until steel yielding. After that, the displacement-controlled loading with an interval of about 300 mm was applied until the failure. The applied load was monitored by a load sensor continuously. Moreover, the strain gauges were adhered to three tensile rebars to monitor their strains at each load interval. During the test, a magnifying glass was used to detect the initiation of cracks in the pure moment zone. The crack widths on the tensile concrete surface of the pure moment zone of the tested beams were measured using a hand-held microscope with an accuracy of 0.01 mm at each load step along with crack number and crack development up to the failure.

3 Crack Width Prediction from Different Codes

3.1 GB 50010, CECS38 and JTG 3362

According to the GB 50010, the maximum crack width of reinforced concrete can be estimated by the following equation. This equation considers the impact of steel reinforcement stress, concrete cover thickness and long-term loading.

$$w_{max} = \alpha_{cr} \psi \frac{\sigma_s}{E_s} l_{cr} \tag{1}$$

where α_{cr} is the member characteristic coefficient relevant to loading characteristics; ψ is the factor considering the non-uniform strain distribution in the steel rebar between the cracks; σ_s is the rebar stress; l_{cr} is the mean crack spacing; E_s is the elastic modulus of the rebar.

The CECS 38 gives the formula to calculate the maximum crack width of fiber-reinforced concrete based

on the model in GB 50010. This formula considers the impact of steel fiber volume and type as well as includes an influence factor β_w of steel fibers on the crack width.

$$w_{f \max} = w_{\max}(1 - \beta_w \lambda_f) \quad (2)$$

where $\beta_w = 0.35$ can be assumed for straight fibers; λ_f is the characteristic value of steel fiber and is equal to $V_f l_f / d_f$; V_f is the volume content of steel fiber; l_f is fiber length and d_f is fiber diameter.

Chinese code JTG/T 3362 (2018) gives the following equation to calculate crack width of reinforced concrete member under flexure and this equation considers the impact of tensile rebar stress, and concrete cover thickness.

$$W_{cr} = C_1 C_2 C_3 \frac{\delta_{ss}}{E_s} \left(\frac{c + d}{0.30 + 1.4 \rho_{te}} \right) \quad (3)$$

where, W_{cr} is the calculated crack width; C_1 is a shape factor of rebar surface, taken as 1.0 for ribbed rebar; C_2 is a long-term factor; C_3 is a characteristic factor for members under different loads, taken as 1.0 for flexural member; δ_{ss} is tensile rebar stress; c is concrete cover thickness; d is tensile rebar diameter; ρ_{te} is effective tensile rebar ratio; E_s is the elastic modulus of the rebar.

Note that the crack widths calculated from Eq. 1–Eq. 3 are at the centroid location of tensile rebars, and thus they need to be transferred to the crack widths on the tensile surface of the tested beams based on the cross-sectional height relationships as follows.

$$w_{s \max} = w_{\max} \left(\frac{h - x}{h_0 - x} \right) \quad (4)$$

where $w_{s \max}$ is the crack width on the beam surface; w_{\max} is the crack width calculated from Eq. 1–Eq. 3; h is the cross-sectional height of the beam; h_0 is the effective height of the beam; x is the compressive height assumed equal to $0.35h_0$.

3.2 NF P18-710

According to the UHPC Standard NF P18-710, for reinforced UHPC members, the crack width at the position of tensile rebar can be calculated as follows. This equation considers the impact of longitudinal tensile rebar stress, tensile rebar bond performance, concrete cover thickness and UHPC tensile strength.

$$w_s = s_{r, \max, f} (\varepsilon_{sm, f} - \varepsilon_{cm, f}) \quad (5)$$

where $s_{r, \max, f}$ is the maximum crack spacing; $\varepsilon_{sm, f}$ is the average strain of the tensile rebar between cracks; $\varepsilon_{cm, f}$ is the average strain of the UHPC between cracks; the

average strain difference between the tensile rebar and UHPC can be calculated below:

$$\begin{aligned} \varepsilon_{sm, f} - \varepsilon_{cm, f} &= \frac{f_{ctfm}}{K_{global} \cdot E_{cm}} \\ &- \frac{1}{E_s} \left[k_t \left(f_{ctfm, el} - \frac{f_{ctfm}}{K} \right) \cdot \left(\frac{1}{\rho_{eff}} + \frac{E_s}{E_{cm}} \right) \right] \end{aligned} \quad (6)$$

$$\rho_{eff} = A_s / A_{c, eff} \quad (7)$$

where δ_s is the stress in the longitudinal tensile rebar at the cracked cross-section; $f_{ctfm, el}$ and f_{ctfm} are the mean tensile limit of elasticity and the mean post-cracking ultimate strength for UHPC, respectively; K_{global} is fiber orientation factor equal to 1.25; k_t is a factor depending on the loading duration or loading repeatability equal to 0.6 for short-term loading in this study; ρ_{eff} is effective reinforcement ratio; A_s is tensile rebar area; $A_{c, eff}$ is the product of effective tensile height (minimum value of $2.5(h-d)$ and $0.5h$; d is cross-sectional effective depth) and cross-sectional width; E_s and E_{cm} are rebar's and UHPC's elastic moduli, respectively.

The maximum spacing between cracks $s_{r, \max, f}$ is calculated using Eq. 8, which includes a concrete cover factor l_0 and a stress transfer length l_t :

$$s_{r, \max, f} = 2.55(l_0 + l_t) \quad (8)$$

$$l_0 = 1.33c / \delta \quad (9)$$

$$l_t = 2 \times \left[0.3k_2 \left(1 - \frac{f_{ctfm}}{K_{global} f_{ctfm, el}} \right) \cdot \frac{1}{\delta \eta} \right] \frac{\phi}{\rho_{eff}} \geq \frac{L_f}{2} \quad (10)$$

$$\delta = 1 + 0.4 \left(\frac{f_{ctfm}}{K_{global} f_{ctfm, el}} \right) \leq 1.5 \quad (11)$$

where, c is the concrete cover for steel rebar; η is a tensile rebar bonding factor equal to 2.25; δ is a parameter which expresses the improvement of the bonding performance of the rebar by the steel fibers in the concrete cover area; k_2 is a factor depending on the strain distribution at the cracked cross-section equal to 0.5 for flexural member (Fig. 4).

Again, the crack width on the tensile surface of UHPC can be calculated from the crack width at the centroid of tensile rebars as follows in Fig. 5, and the following equation also applies to the surface crack width calculation by the MC method introduced next.

$$w_t = w_s (h - x_0 - x) / (d - x_0 - x) \quad (12)$$

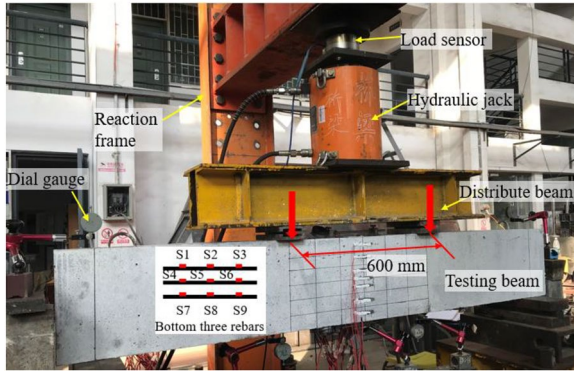


Fig. 4 Flexural test setup

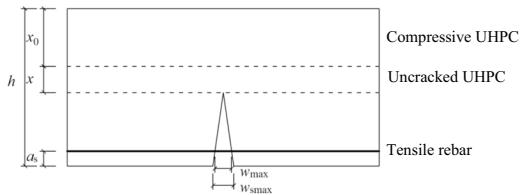


Fig. 5 Crack width calculation transformation to the surface

where h is the entire height of the cross-section; d is the effective height of the cross-section; x_0 is the height of the compression zone; x is the height of the uncracked cross-section at the tension zone (i.e., tensile stress smaller than tensile strength).

3.3 MC

In the MC, the maximum crack width at the center of steel rebars is calculated according to the following equations. The transfer length and the maximum steel stress at a crack in the crack initiation phase are modified in accordance with the crack width prediction of normal concrete.

$$w_d = 2l_{s,max}(\varepsilon_{sm} - \varepsilon_{cm} - \varepsilon_{cs}) \quad (13)$$

$$l_{s,max} = k \cdot c + \frac{1}{4} \frac{(f_{ctm} - f_{Ftsm})}{\tau_{bm}} \frac{\phi_s}{\rho_{s,ef}} \quad (14)$$

$$\varepsilon_{sm} - \varepsilon_{cm} - \varepsilon_{cs} = \frac{\delta_s - \beta \cdot \delta_{sr}}{E_s} - \eta_r \varepsilon_{sh} \quad (15)$$

$$\delta_{sr} = \frac{f_{ctm} - f_{Ftsm}}{\rho_{s,ef}} (1 + \alpha_e \rho_{s,ef}) \quad (16)$$

where $l_{s,max}$ is the length where slip between concrete and steel rebar occurs; ε_{sm} is the mean steel rebar strain over $l_{s,max}$; ε_{cm} is the mean concrete strain over $l_{s,max}$; ε_{cs}

is the concrete free shrinkage strain; k is an empirical factor considering the effect of the concrete cover equal to 1.0; c is the concrete cover thickness; ϕ_s is the diameter of steel rebar; $\rho_{s,ef}$ is the effective ratio of steel rebar and $\rho_{eff} = A_s/A_{c,eff}$; A_s is the area of steel rebar; $A_{c,eff}$ is the effective area of concrete in tension; f_{ctm} is the average concrete tensile strength; f_{Ftsm} is the average value of serviceability residual strength (i.e., post-cracking residual strength); τ_{bm} is the mean bond strength between rebar and concrete and $\tau_{bm} = 1.8f_{ctm}$ can be assumed; δ_s is the stress of steel rebar at the cracked cross-section; δ_{sr} is the maximum stress of steel rebar in the crack initiation stage; β is an empirical factor to evaluate average stress over $l_{s,max}$ which is related to the loading type; η_r is a factor considering the contribution of shrinkage; ε_{sh} is the shrinkage strain; E_s is the modulus of elasticity of steel; α_e is the modulus ratio of E_s/E_c .

3.4 Rebar Stress

From above crack width calculation equations, it is noted that the rebar stress is of importance for accurate crack width prediction and affects calculation results. In accordance with GB50010, the rebar stress at the cracked cross-section can be calculated as follows.

$$\delta_s = \frac{M_s}{\eta A_s h_0} \quad (17)$$

where, δ_s is the tensile rebar stress; M_s is the measured bending moment; η is a force arm coefficient taken as 0.87; A_s is a tensile rebar cross-sectional area; h_0 is an effective height of the cross-section.

3.5 Modified Crack Width Prediction Based on GB50010-2010

3.5.1 Rebar Stress

To consider the crack width impact on the durability and service life of the structure, rebar stress is calculated till the crack width of 0.20 mm after which the cracks propagate quickly for UHPC beams. Fig 6 shows the simplified stress diagram of the cracked cross-section at the serviceability limit state, and several assumptions are made to facilitate the rebar stress calculation as follows: (1) plane cross-section assumption is satisfied; (2) the tensile contribution from the UHPC is considered and an equivalent tensile block with a strength value of $0.8 f_{tk}$ is assumed (f_{tk} —the tensile strength); (3) at the serviceability limit state, elastic UHPC is assumed at the compressive zone with a triangle stress diagram, and the tensile rebars do not yield and are in linear elastic stage prior to the crack width of 0.20 mm from the experimental observations.

Based on force and moment equilibriums on the cross-section in Fig. 6 along with cross-sectional parameters,

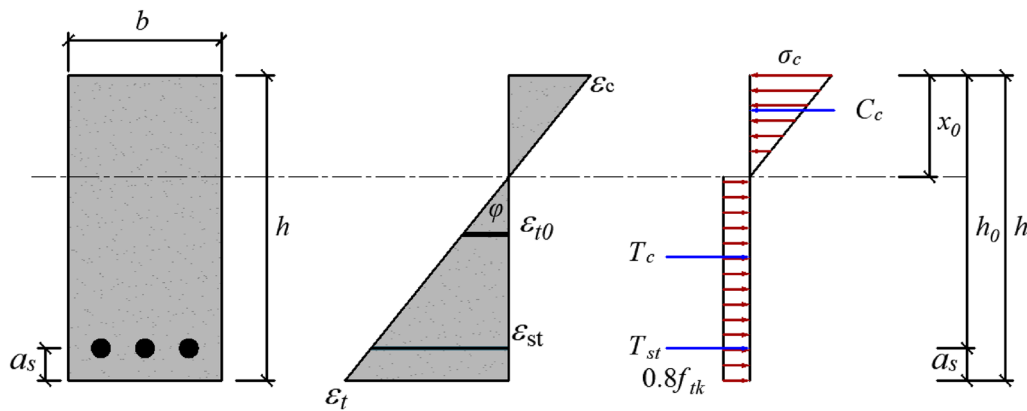


Fig. 6 Stress-strain diagram on the cross-section for rebar stress calculation

tensile rebar area, and UHPC tensile strength, the cross-sectional curvature ϕ and compressive zone height x_0 can be solved as below (two equations of equilibrium for two unknowns), and the rebar stress can be calculated, based on the known strain distribution.

$$\sum N = 0, C_{UHPC} = T_{UHPC} + T_s \quad (18)$$

$$\sum M = 0, 0 = M_c + M_t + M_s \quad (19)$$

$$C_{UHPC} = \frac{1}{2} E_c \phi x_0^2 b \quad (20)$$

$$T_{UHPC} = 0.8 f_{tk} (h - x_0) b \quad (21)$$

$$T_s = \delta_s A_f \quad (22)$$

$$M_c = \frac{2}{3} x_0 \cdot C_{UHPC} = \frac{1}{3} E_c \phi x_0^3 b \quad (23)$$

$$M_t = T_{UHPC} \cdot \frac{h - x_0}{2} = 0.8 f_{tk} b \frac{(h - x_0)^2}{2} \quad (24)$$

$$M_s = T_s \cdot (h_0 - x_0) = \delta_s A_f (h_0 - x_0) \quad (25)$$

$$\delta_s = E_s (h_0 - x_0) \phi \quad (26)$$

where C_{UHPC} is the axial force of UHPC at the compression zone; T_{UHPC} is the axial force of UHPC at the tension zone; T_s is the axial force of tensile steel reinforcement.

3.6 Average Crack Spacing

In accordance with GB50010, the average crack spacing can be calculated as follows.

$$l_{cr} = 1.9 c_s + 0.08 \frac{d_{eq}}{\rho_{te}} \quad (27)$$

where, c_s is the concrete cover thickness; ρ_{te} is the tensile rebar ratio from effective tensile concrete cross-section area (A_{te}), $\rho_{te} = A_s / A_{te}$; d_{eq} is the equivalent diameter of the tensile rebar.

Since steam-cured UHPC shows dense microstructure with low porosity and defects and is reinforced with steel fibers with excellent tensile performance, the fiber-bridging capacity provides residual tensile strength, connects crack surfaces, and transfers tensile stress at cracks. As a result, the crack distribution becomes more uniform and the crack spacing is shortened as compared to normal reinforced concrete. Moreover, the average crack spacing reduces more as the reinforcement ratio and fiber volume increase. The steel fiber reinforcement in the matrix can be regarded as many small steel reinforcements connecting cracks due to the fiber-matrix bond to reduce crack spacing. Based on the above discussion, it is necessary to modify the average crack spacing as follows since the Eq. 27 defined in the GB50010 does not consider the impact of steel fibers.

$$l_{cr'} = \frac{\alpha}{1 + \beta \lambda_f} \times \left(0.81 c_s + 0.08 \frac{d_{eq}}{\rho_{te}} \right) \quad (28)$$

where, λ_f is characteristic coefficient of steel fibers and can be calculated by $\lambda_f = \rho_f / \beta$; β is fiber distribution influence factor and taken as 0.5; α is another influence

factor affecting average cracking spacing and taken as 1.65 for the steel fibers (length of 13 mm, diameter of 0.2 mm and volume content of 2%, for example). The crack spacing is related to fiber volume and aspect ratio, and the regression analysis from the test data is needed to obtain the coefficients of this equation.

3.7 Nonuniformity Distribution Coefficient of Rebar Strain

The nonuniformity distribution coefficient of longitudinal rebar strain can be calculated as follows in accordance with GB50010. It is defined by the ratio of the average strain of rebar between cracks to the maximum strain of the rebar at the cracked section.

$$\psi = 1.1 - 0.65 \frac{f_{tk}}{\rho_{te}\sigma_s} \quad (29)$$

where, f_{tk} is the characteristic value of axial tension strength of concrete.

For normal concrete, the residual tensile strength is low and can be neglected. The rebar carries large force and shows large strain at the cracked cross-section. The nonuniformity distribution coefficient of rebar is relatively small in the normal concrete. However, for UHPC, due to excellent tensile performance and ductility and delayed crack development, the rebar strain is reduced at the cracked cross-section and the rebar strain distribution becomes more uniform in the pure bending moment region. It is expected that the nonuniformity distribution coefficient of rebar strain in the UHPC is greater than that in the normal concrete considering the contribution of steel fibers. During the experimental test, nine strain gauges were attached to the rebars in the pure bending moment region of the tested beams to record their strains and the measured nonuniformity coefficient values of rebar strain can be obtainable. Then, a modified nonuniformity distribution equation is regressed based on the test data as follows.

$$\psi' = 1.1 - 0.24 \frac{f_{tk}}{\rho_{te}\sigma_s} \quad (30)$$

If the calculated value is greater than 1, the value is taken as 1; if the calculated value is smaller than 0.5, the value is taken as 0.5.

3.8 Member Characteristic Coefficient

The member characteristic coefficient can be calculated as follows.

$$\alpha_{cr} = \tau_0 \tau_1 \beta \alpha_c \quad (31)$$

where, τ_0 is an influence factor of long-term load effect and τ_0 is taken as 1 in this study because steam cured UHPC usually exhibits neglected shrinkage and creep under long-term loading; τ_1 is a ratio of the maximum crack width to the average crack width and the ratio generally reflects the influence of the uneven crack width distribution, taken as 1.66, depending on the loading characteristics (such as axially tensioned, flexural and eccentrically tensioned members); β is an influence factor of crack spacing, taken as 1.0; α_c is a factor related to the influence of concrete elongation between cracks, taken as 0.85 in accordance with GB50010, depending on the loading characteristics rather than structural materials.

3.9 Modified Crack Width Prediction

Based on the above discussion, the maximum crack width at the rebar centroid of the UHPC beam can be calculated as follows. Similarly, the maximum crack width on the tensile surface of the beam can be calculated from the Eq. 12 and compared with the measured results.

$$w_{\max} = \alpha_{cr} \psi' \frac{\sigma_s}{E_s} l_{cr'} \quad (32)$$

where, different parameters and coefficients can be calculated based on the modified equations above.

4 Results and Discussion

4.1 Crack Width Prediction from Existing Codes

Fig 7 shows the experimental and predicted crack widths of the tested beams from existing codes. Under each load, we recorded crack numbers and widths and uploaded these data as a supplementary file. After crack width is greater than 0.05 mm, the predicted crack widths from GB 50010 are significantly more than the experimental ones, and the errors increase with load. JTG 3362 always overestimates crack width. Conservative crack width predictions are made from normal concrete codes. For CECS 38, the predictions are generally smaller than the test ones, especially for the beams with large fiber volume or reinforcement ratio. Although CECS 38 equation considers steel fiber improvement on crack width and introduces an influencing factor with a constant value for this reinforcement, the impact of steel fiber volume content and reinforcement ratio is not considered explicitly and thus, the errors between them are still observed. MC first overestimates crack width until about 0.1 mm, and then underestimates crack width. For AFGC, the predicted crack widths are relatively close to the experimental ones, but still in the safety side. The errors between them are increasing for the beams with large fiber volume or low reinforcement ratio.

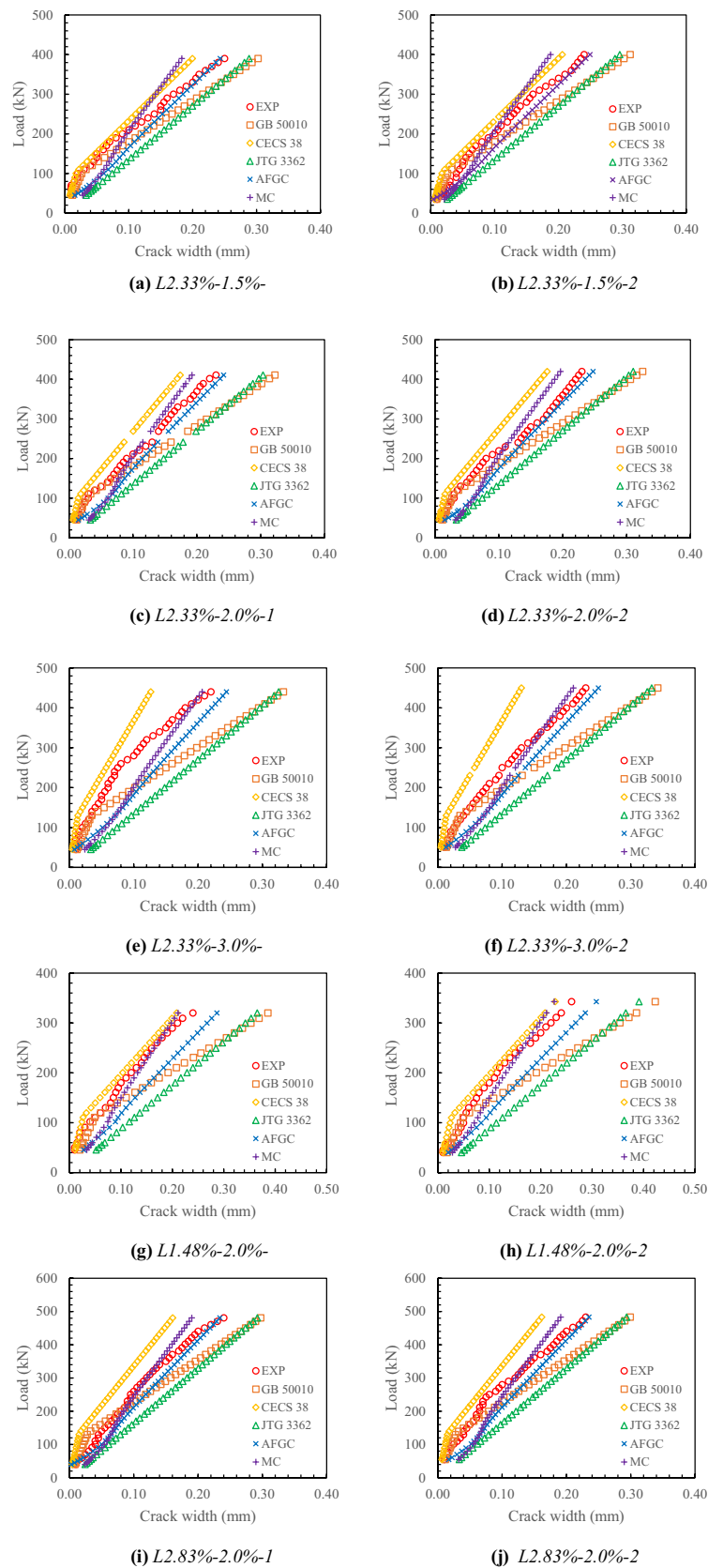


Fig. 7 Comparisons between the experimental crack widths and the predicted crack widths from different codes

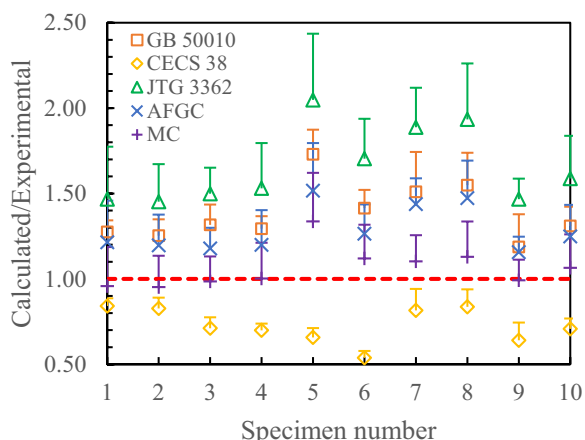


Fig. 8 Average value of ratios of calculated to experimental crack width at different loads of each specimen (specimen number 1~8 corresponds to specimen number a~j in Fig. 7)

To quantify the differences between the predicted and experimental crack widths of the tested beams, average value, and standard deviation of the ratios of the predicted to experimental crack widths at different loads of each specimen are statistically calculated to highlight the modification need of existing codes. Note that for these statistic quantities, the crack width ranges between 0.05 mm and 0.25 mm since the initial crack width counted is about 0.05 mm and the crack propagation accelerates after 0.25 mm. Fig 8 shows the average ratio of each specimen along with the standard deviation. The specimen number of the horizontal axis represents the ten tested beams following the exact specimen order in Fig. 7 for clarity.

From Fig. 8, GB 50010 gives an average value of 1.38 and standard deviation of 0.13 for the ratios of the predicted to experimental crack widths of all specimens, while JTG 3362 exhibits an average value of 1.66 and standard deviation of 0.25, which indicates that the normal concrete codes show conservative predictions with high scattering. For CECS 38, the average value is 0.73 and standard deviation is 0.07 for the ratios of all specimens; the predictions are smaller than the experimental ones, providing unsafe estimations. For MC, the average value is 1.06, which is close to 1, but the standard deviation is 0.19 with relatively high scattering. This is attributed to the large predictions at the beginning and the small predictions at the later stage. AFGC shows the average value of 1.29 and the standard deviation of 0.18, and the predictions are greater than the experimental ones again, especially in the tested beams with large fiber volume or low reinforcement ratio. Although AFGC shows smaller average value than the normal concrete codes, large scattering can still be observed.

Generally, the normal concrete codes show unreasonable crack width predictions of the UHPC beams.

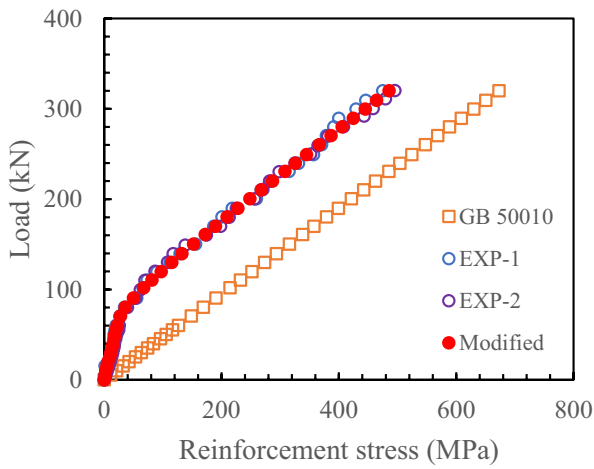
Although CECS 38 considers the impact of steel fiber with introducing a constant modification coefficient, as the load increases, UHPC tensile strength gradually decreases, and the restraint effect from steel fibers weakens. As a result, the predicted errors from CECS 38 are increasing. MC and AFGC consider the influence of UHPC tensile strength on the crack width prediction, but the errors increase unsafely after a certain crack width. Moreover, they include many parameters for prediction and are not friendly for engineering applications. However, GB 50010 considers main influencing factors, and they have clear physical meanings, easing analysis. Although steel fibers in UHPC beam hinder crack width development, crack width intrinsically depends on the strain difference between UHPC and longitudinal rebar, which has been reflected in GB 50010 equations. Therefore, this study modifies equations in GB 50010 for crack width prediction of UHPC beam in combination with the test data.

4.2 Rebar Stress

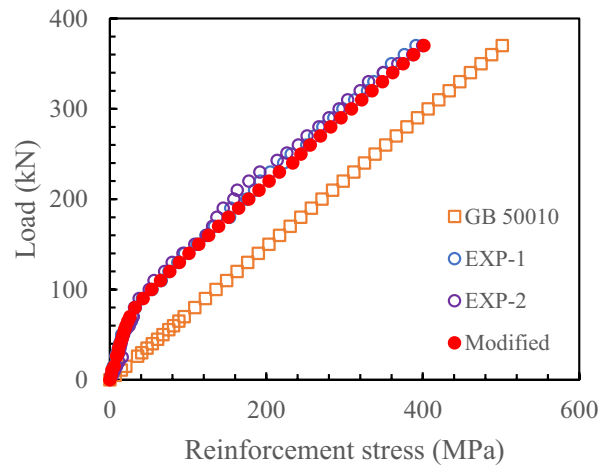
Fig 9 shows the experimental and predicted rebar stresses from Eq. 17. It is found that GB 50010 significantly overestimates the rebar stresses of the tested beams. This is attributed to the fact that the fiber bridging capacity equips UHPC with high residual tensile strength at the cracks. Fig 9 also shows the re-calculated rebar stresses from Eq. 26, considering UHPC contribution at the cracks. Overall, the proposed rebar stress analysis with considering residual tensile strength of UHPC shows reasonable predictions compared to the experimental stresses.

4.3 Average Crack Spacing

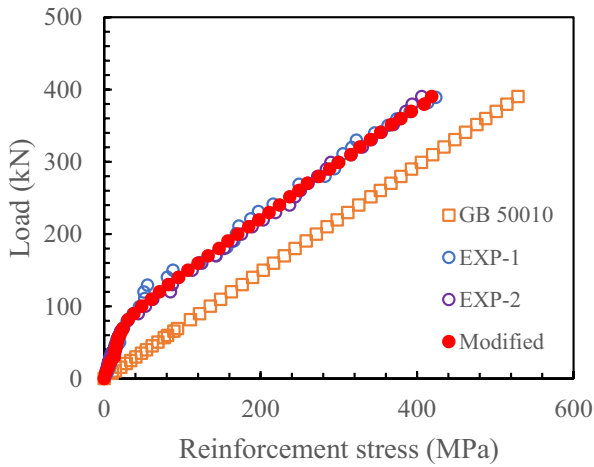
The average crack spacing has an important influence on the crack width development. During the test, the number of cracks was recorded along with crack width and length to obtain average crack spacing at each load level after beam cracked. Table 2 shows experimental crack spacings of different steel reinforced UHPC beams. As the fiber volume increases, the number of cracks increases while average crack spacing decreases; for example, at the serviceability stage of 0.2 mm, the average crack spacing is increased by 26% with fiber volume decreasing from 3% to 1.5%. This is attributed to the fact that the use of steel fibers increases post-cracking tensile performance of UHPC, which carries partial of the external load and restrains the overall deformation. On the other hand, the formation of the mechanical anchorage between the rebar ribs and randomly distributed steel fibers reduces the strain difference between the rebar and UHPC, resulting in a more even crack distribution and



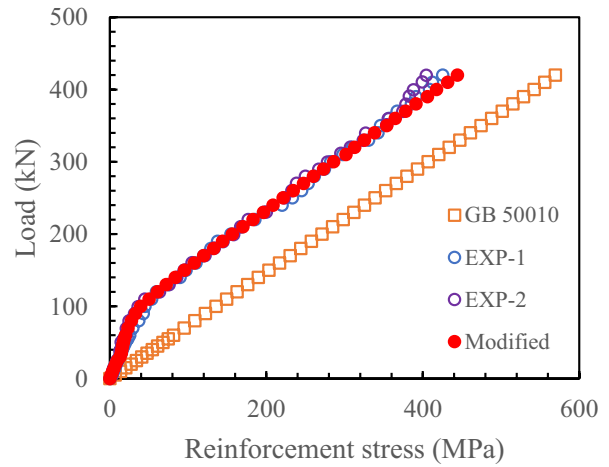
(a) 1.48%-2.0%



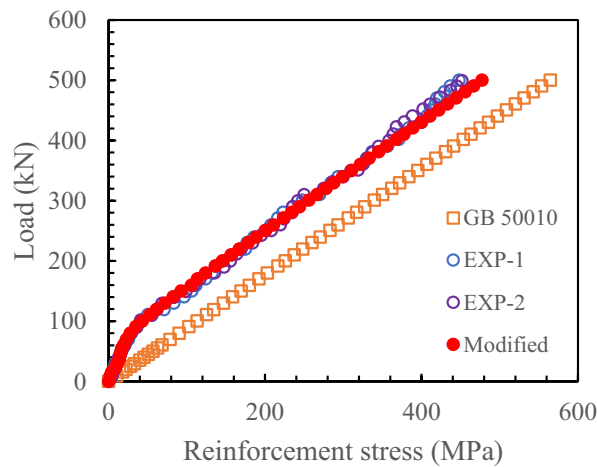
(b) 2.33%-1.5%



(c) 2.33%-2.0%



(d) 2.33%-3.0%



(e) 2.83%-2.0%

Fig. 9 Comparisons between the predicted and experimental rebar stresses

Table 2 Experimental crack spacing in this study

Specimens	$W_{max}=0.05$ (mm)	Average	$W_{max}=0.10$ (mm)	Average	$W_{max}=0.20$ (mm)	Average
L2.33%-1.5%-1	62.40	56.60	47.10	40.20	29.10	25.05
L2.33%-1.5%-2	50.80		33.30		21.00	
L2.33%-2.0%-1	63.30	58.30	30.90	30.65	23.90	21.7
L2.33%-2.0%-2	53.30		30.40		19.50	
L2.33%-3.0%-1	45.10	48.35	30.10	31.2	18.50	19.85
L2.33%-3.0%-2	51.60		32.30		21.20	
L1.48%-2.0%-1	78.30	82.45	26.00	27.5	24.50	24.20
L1.48%-2.0%-2	86.60		29.00		23.90	
L2.83%-2.0%-1	45.40	51.45	21.40	22.55	18.70	18.80
L2.83%-2.0%-2	57.50		23.70		18.90	

Table 3 Quantitative comparison between measured and predicted crack spacings

Average crack spacing (mm)							
Specimens	Crack numbers	Measured①	Average	Equation 27 Predicted②	Equation 28 Predicted③	②/①	③/①
L2.33%-1.5%-1	10	66.67	63.33	76.22	60.36	1.20	0.95
L2.33%-1.5%-2	11	60.00					
L2.33%-2.0%-1	12	54.55	52.27	76.22	54.42	1.46	1.04
L2.33%-2.0%-2	13	50.00					
L2.33%-3.0%-1	13	50.00	48.08	76.22	47.59	1.59	0.99
L2.33%-3.0%-2	14	46.15					
L1.48%-2.0%-1	11	60.00	63.33	85.76	63.96	1.35	1.01
L1.48%-2.0%-2	10	66.67					
L2.83%-2.0%-1	13	50.00	50.00	72.74	50.95	1.45	1.02
L2.83%-2.0%-2	13	50.00					
Standard deviation						0.13	0.03
Average						1.41	1.00
Coefficient of variance						0.09	0.03

smaller average crack spacing. As the reinforcing ratio increases, the average crack spacing decreases; for example, the average crack spacing increases by 29% with reinforcing ratio decreasing from 2.83% to 1.48%, mainly due to the smaller rebar stress (or strain) and strain difference from concrete at higher reinforcing ratio, slowing down the crack width development. Table 3 statistically shows the experimental and predicted average crack spacings. For analyzing experimental crack spacings, the visible crack widths greater than 0.05 mm are counted since the crack width of less than 0.05 mm (i.e., microcrack) does not impact the durability of UHPC members. From Table 3, the predicted crack spacings from GB 50010 are greater than the measured ones, and the errors increase for the beams with large fiber volume. With the use of the calibrated equation, the average value of the ratios of the predicted to experimental crack spacings of different

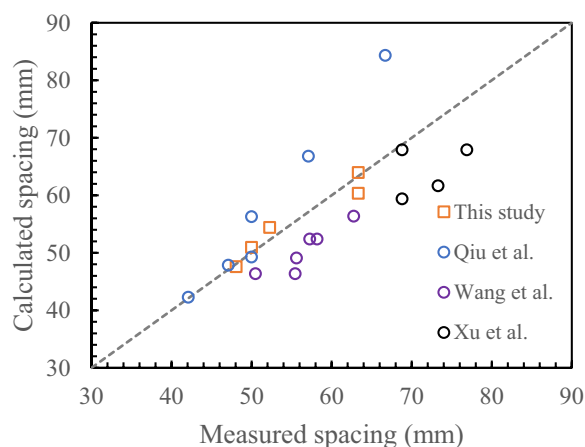
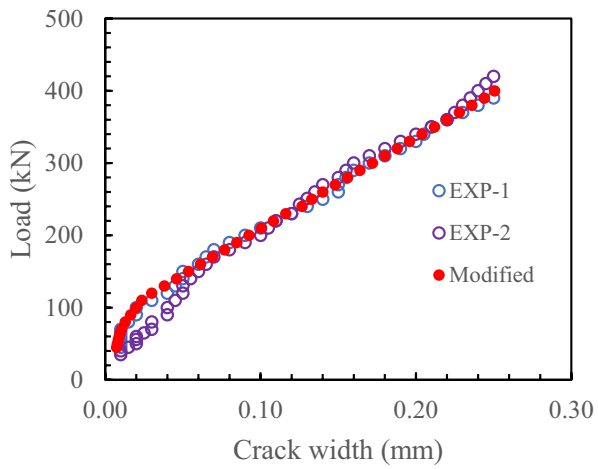
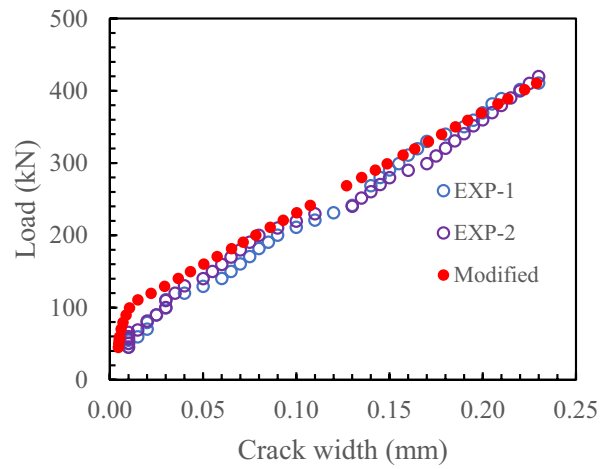


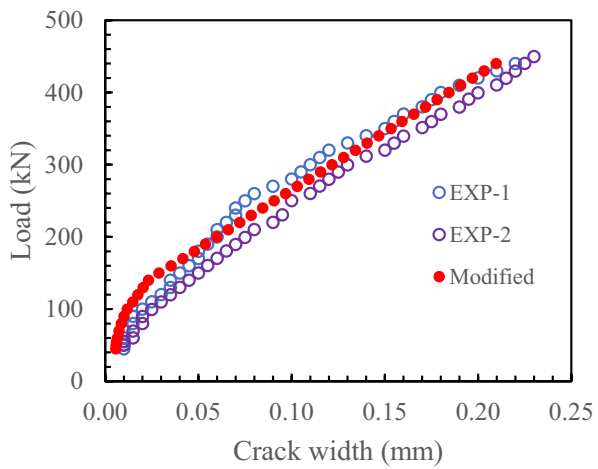
Fig. 10 Visualization of measured and predicted average crack spacing comparison



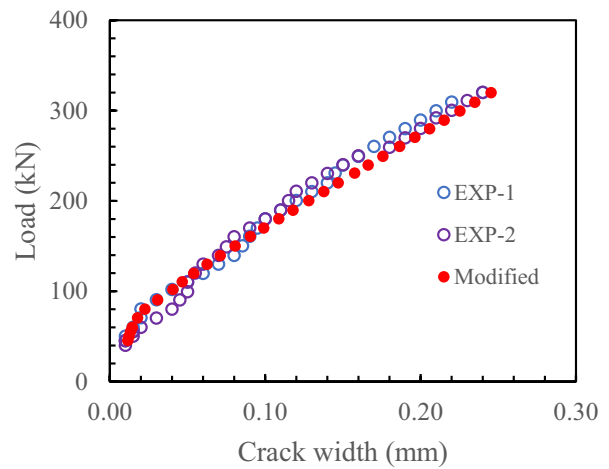
(a) *L2.33%-1.5%*



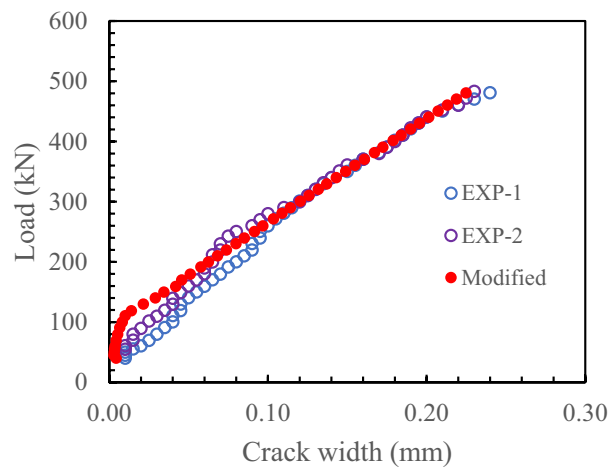
(b) *L2.33%-2.0%*



(c) *L2.33%-*



(d) *L1.48%-2.0%*



(e) *L2.83%-2.0%*

Fig. 11 Comparisons of experimental and predicted crack width from the modified equations

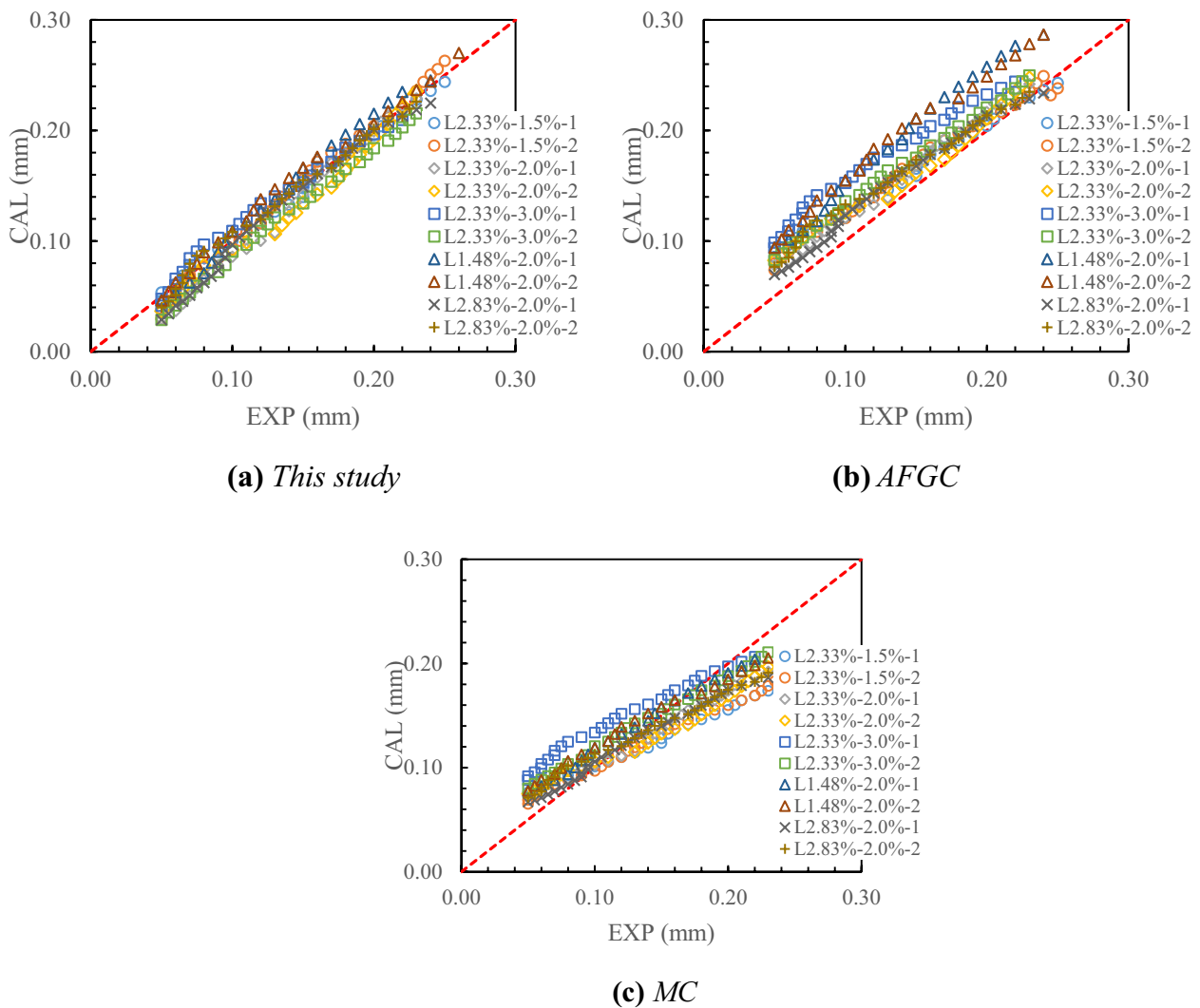


Fig. 12 Direct comparisons between the experimental and predicted crack width from modified equation, AFGC and MC

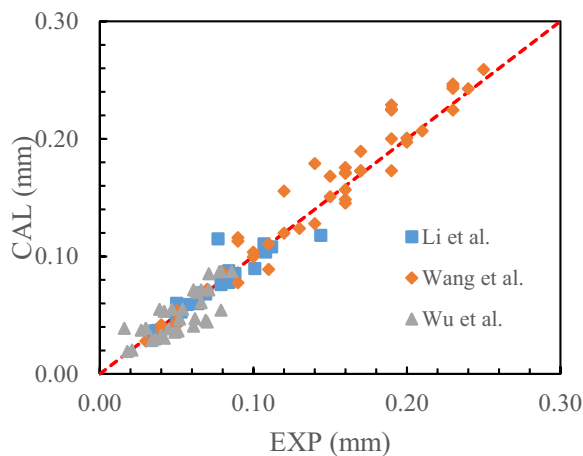


Fig. 13 Crack width prediction in other studies using modified equation

specimens is 1.00, along with the standard deviation of 0.03.

To further verify the accuracy of the modified crack spacing equation, fifteen UHPC beams in the literature are selected for average crack spacing calculation, and the predicted crack spacings are compared with the measured ones as shown in Fig. 10. For Qiu et al.'s study (2020), the errors are higher than 15% for two tested beams with small reinforcement ratios. Also, crack width readings from human may induce additional errors. For Wang et al.'s study (2017), the predicted crack spacings are smaller than the measured ones since their UHPC includes coarse aggregate, increasing pores and defects and reducing tensile cracking strength and performance. The modified crack spacing in this study is based on the UHPC with fine aggregate, which may make smaller crack spacing predictions than the measured ones. Xu

Table 4 Key properties of the experimental measured outcomes

Specimens	Rebars	Cover thick (mm)	Cross-sectional size (mm ²)	Rebar area (mm)	Rebar ratio	Tensile strength UHPC	Elastic modulus UHPC
B-1	4Φ20	20	350×160 Wang et al., (2017)	1256	0.0513	14.1 MPa	59 GPa
B-2		20		1256	0.0513		
B-5		20		1256	0.0513		
B-6		20		1256	0.0513		
C-1	6Φ16	20		1206	0.0492		
C-4		20		1206	0.0492		
C-6		20	1206	0.0492			
C-8		20	1206	0.0492			
D-2	4Φ18	20		1018	0.0416		
D-3		20		1018	0.0416		
D-6		20		1018	0.0416		
E-1	4Φ22	20		1520	0.0620		
L1	2Φ25	20	150×250 Wu et al., (2014)	982	0.0524	7.6 MPa	42 GPa
L2	3Φ25	20		1473	0.0786		
L3	4Φ25	20		1964	0.1047		
L4	2Φ25+2Φ18	20		982	0.0524		
L5	2Φ25	20		982	0.0524		
L6	2Φ25+2Φ16	20		1384	0.0738		
L7	2Φ25	20		982	0.0524		
L8	2Φ18+2Φ16	20		911	0.0486		
L-2	2Φ14	25	150×200 Li et al., (2010)	308	0.0210	10.2 MPa	48.1 GPa
L-3	2Φ22	25		760	0.0510		
L-4	3Φ18	25		763	0.0510		
L-5	2Φ25+1Φ22	25		1362	0.0910		
L-6	2Φ22+1Φ40	25		2017	0.1340		

et al.'s study (2015) used prestressing strands and high-strength steel rebar, which is different from the rebars used in this study and may result in prediction errors. Generally, the predictions agree well with the experimental results from the modified crack spacing equation along with the average value of 0.97 and the standard deviation of 0.12 for the data in these studies.

4.4 Modified Crack Width

Fig 11 shows comparisons between the predicted and experimental crack widths of the tested beams. It is found that the modified crack width equations provide reasonable crack width development predictions of the tested UHPC beams. For the crack width smaller than 0.05 mm, the predicted crack widths are smaller than the experimental ones. This may be attributed to that at this load with small width value, the tensile stress in the UHPC did not drop significantly due to strain hardening behavior and the strain difference between the UHPC and rebar at

the crack was not high. However, the Eq. 30 gives a small nonuniformity distribution coefficient of rebar strain at this load, leading to smaller predictions.

Fig 12 presents more direct crack width comparisons predicted by the modified equation in this study and two existing codes to demonstrate the accuracy of the proposed equation. Clearly, AFGC provides conservative crack width predictions with large scattering; for MC, the calculated crack widths are greater than the experimental ones first. They are gradually decreasing with the load and the errors increase again. The modified equation in this study shows good agreement along with smaller scattering than AFGC and MC, along with the average value of 0.97 and the standard deviation of 0.11 for all the data from the test beams.

Since the experimental tests are subjected to the short-term load, some of discussion related to the long-term effect may be of interest to the readers. Under the long-term load, the crack width may further expand due to concrete shrinkage and creep.

Steam-cured UHPC usually does not have later shrinkage and has smaller creep coefficient than normal concrete with the addition of steel fibers (Garas et al., 2009; Graybeal, 2006). The impact of the long-term load on the crack width prediction may be reduced. If the influencing factor of the long-term load is selected from GB 50010, the modified equation is capable of safely predicting crack width for UHPC members in practical engineering applications.

Fig 13 shows the applicability validation of the modified equation for predicting crack width in other studies, and the key properties of the experimental measured outcomes are listed in Table 4. Crack width test data from twenty-five UHPC beams under flexure are collected, 20 pairs of data of five beams in Li et al.'s study (2010), 48 pairs of data of twelve beams in Wang et al.'s (2017) study, and 32 pairs of data of eight beams in Wu et al.'s study (2014). Fig 13 shows the comparisons between the predicted and experimental crack widths of the UHPC beams. Overall, the modified equation is promising to predict crack width accurately along with the average value of 1.03 and the standard deviation of 0.21 from these validated data.

5 Conclusions

This study investigates the flexural cracking behavior of steel reinforced UHPC beams with different steel reinforcing ratios and fiber volumes. Existing relevant codes are applied to predict crack width of these beams and the predicted crack widths are compared with the tested ones. Modified crack width prediction equations with calibrated coefficients are developed, based on Chinese code GB50010, and following conclusions are drawn.

- From experimental observations, multiple cracking behavior and localized crack are further confirmed in the steel reinforced UHPC beams. Although both increasing steel reinforcing ratio and fiber volume reduce average crack spacing along with more even distribution of cracks, steel reinforcing ratio shows better improvement effectiveness in controlling crack width development.
- Normal concrete codes (GB50010 and JTG 3362) show conservative crack width predictions with high scattering. Although CECS 38 generally underestimates crack width and MC underestimates crack width after 0.1 mm, the predictions from AFGC are in the safety side, especially for the beams with large fiber volume and low reinforcement ratio.
- The residual tensile strength of UHPC shows an important influence on the rebar stress calculation in the mechanics-based model. The residual tensile

strength of is $0.8 f_{tk}$ for the equivalent stress block shows accurate rebar stress predictions.

- With the calibrated equations for calculating average crack spacing and nonuniformity distribution coefficient of rebar strain, the modified crack width equation shows prediction accuracy of 0.97–1.03 and standard deviation of 0.11–0.21 in this study and other investigations. Therefore, the modified equations are expected to be validated in future studies to promote structural design and crack control of steel reinforced UHPC beams.

Supplementary Information

The online version contains supplementary material available at <https://doi.org/10.1186/s40069-023-00628-x>.

Additional file 1. Crack number and width data.

Acknowledgements

This research is sponsored by the National Natural Science Foundation of China (Grant No. 52078200) and the Science Research Project of Education Department of Hunan Province (Grant No. 21A0019).

Author contributions

The first author, YZ collected data from the experiments, designed the work, conducted data analyses, and drafted the manuscript. The second author, YZ supervised the project, proposed conception, and contributed to design of the work. The third author, XY participated in the revision of the manuscript. The fourth author, CH participated in the experimental test and data collection, and designed the work. All authors read and approved the final manuscript.

Funding

This research is sponsored by the National Natural Science Foundation of China (Grant No. 52078200) and the Science Research Project of Education Department of Hunan Province (Grant No. 21A0019).

Availability of data and materials

The data sets used and/or analyzed during the current study are available from the corresponding author on reasonable request.

Declarations

Competing interests

The authors declare that they have no competing interests.

Received: 31 January 2023 Accepted: 8 August 2023

Published online: 26 December 2023

References

- Borosnyoi, A., & Balazs, G. L. (2005). Models for flexural cracking in concrete: the state of the art. *Structural Concrete*, 6(2), 53–62.
- Brühwiler E (2017) Strengthening of existing structures using R-UHPFRC: principles and conceptual design. The 2ndACF Symposium, Innovations for Sustainable Concrete Infrastructures(1): 993–1002.
- CEB-FIP. Model code for concrete structures 2010. International Federation for Structural Concrete, Lausanne.
- CECS 38. Technical specification for fiber reinforced concrete structures. Beijing, China, 2004.

- Chen, S., Zhang, R., Jia, L. J., et al. (2018). Flexural behaviour of rebar-reinforced ultra-high-performance concrete beams. *Magazine of Concrete Research*, 70(19), 997–1015.
- CNR-DT 204/2006. Guide for the design and construction of fiber-reinforced concrete structures. Italian National Research Council, Rome, Italy.
- de Larrard, F., & Sedran, T. (1994). Optimization of ultra-high-performance concrete by the use of a packing model. *Cement and Concrete Research*, 24(6), 997–1009.
- Feng, Z., Li, C., Yoo, D. Y., et al. (2021). Flexural and cracking behaviors of reinforced UHPC beams with various reinforcement ratios and fiber contents. *Engineering Structures*, 248, 113266.
- Garas, V. Y., Kahn, L. F., & Kurtis, K. E. (2009). Short-term tensile creep and shrinkage of ultra-high performance concrete. *Cement and Concrete Composites*, 31(3), 147–152.
- GB 50010–2010. Code for design of concrete structures. Beijing, China, 2010.
- Graybeal B (2006) Material Property Characterization of Ultra-high Performance Concrete. 6300 Georgetown Pike, McLean, VA 22101–2296, USA: Federal Highway Administration. (Report no. FHWA-HRT-06–103).
- Graybeal, B., & Baby, F. (2013). Development of direct tension test method for ultra-high-performance fiber-reinforced concrete. *ACI Materials Journal*, 110(2), 177–186.
- Habel, K., Denari'e, E., & Brühwiler, E. (2007). Experimental investigation of composite ultra-high-performance fiber-reinforced concrete and conventional concrete members. *ACI Structural Journal*, 104(1), 93–101.
- Hasgul, U., Turker, K., Birol, T., et al. (2018). Flexural behavior of ultra-high-performance fiber reinforced concrete beams with low and high reinforcement ratios. *Structural Concrete*, 19(6), 1577–1590.
- Hong, S., Ko, W. J., & Park, S. K. (2013). New analytical approach of flexural crack width estimation for reinforced concrete beams. *Advances in Structural Engineering*, 16(10), 1763–1777.
- Hussein, H. H., Sargand, S. M., Zhu, Y. P., et al. (2022). Experimental and numerical investigation on optimized ultra-high performance concrete shear key with shear reinforcement bars. *Structures*, 40, 403–419.
- JTG/T 3362–2018. Specification for design of highway reinforced concrete and prestressed concrete bridge and culverts, Beijing. [In Chinese.]
- Leutbecher T, Fehling E. Tensile behavior of ultra-high-performance concrete reinforced with reinforcing bars and fibers: Minimizing fiber content. *ACI Struct J*. 2012;109(2):253–263.
- Li L (2010) Study on mechanical performance and design method of reactive powder concrete beams, PhD thesis, Harbin Institute of Technology.
- Meng, W., & Khayat, K. H. (2016). Mechanical properties of ultra-high-performance concrete enhanced with graphite nanoplatelets and carbon nanofibers. *Composites Part B: Engineering*, 107, 113–122.
- Meng, W., & Khayat, K. H. (2018). Effect of graphite nanoplatelets and carbon nanofibers on rheology, hydration, shrinkage, mechanical properties, and microstructure of UHPC. *Cement and Concrete Research*, 105, 64–71.
- NF P 18–710. National addition to Eurocode 2 - Design of concrete structures: specific rules for ultra-high-performance fibre-reinforced concrete (UHP-FRC). Francis de Pressensé, France, 2016.
- Piyasena, R., Loo, Y. C., & Fragomeni, S. (2004). Factors influencing spacing and width of cracks in reinforced concrete; new prediction formulae. *Advances in Structural Engineering*, 7(1), 49–60.
- Qi, J., Wang, J., & Ma, Z. J. (2018). Flexural response of high-strength steel-ultra-high-performance fiber reinforced concrete beams based on a meso-scale constitutive model: experiment and theory. *Structural Concrete*, 19(3), 719–734.
- Qiu, M. H., Shao, X. D., Hu, W. Y., et al. (2020b). Calculation method for crack width of reinforced UHPC flexural components. *China Civil Engineering Journal*, 53(10), 89–98.
- Qiu, M. H., Shao, X. D., Zhu, Y. P., et al. (2020a). Experimental investigation on flexural cracking behavior of ultrahigh performance concrete beams. *Structural Concrete*, 21(5), 2134–2153.
- Qiu, M. H., Shao, X. D., Zhu, Y. P., et al. (2022). Effect of aspect ratios of hooked end and straight steel fibers on the tensile strength of UHPFRC. *Journal of Materials in Civil Engineering*, 34(7), 04022131.
- Richard P and Cheyrez MH (1994) Reactive Powder Concretes with High Ductility and 200–800 MPa Compressive Strength. Indianapolis, IN: American Concrete Institute, ACI Special Publication SP-144, 507–518.
- RILEM 162-TDF. (2003) Test and design methods for steel fiber reinforced concrete σ - ϵ design method - final recommendation. *Materials and Structures* 36:560-567.
- Wang C (2017) Experimental study on flexural performance of ultrahigh performance concrete structures, PhD thesis, Southwest Jiaotong University.
- Wille, K., El-Tawil, S., & Naaman, A. E. (2014). Properties of strain hardening ultra high performance fiber reinforced concrete (UHP-FRC) under direct tensile loading. *Cement and Concrete Composites*, 48, 53–66.
- Wu X (2014) Experimental study on cracking performance of normal cross-section of RPC reinforced with high strength steel rebar, PhD thesis, Guilin University of Technology.
- Xu H (2015) Mechanical performance research on HRB500 steel and prestressing strand reinforced ultrahigh performance concrete beams, PhD thesis, Beijing University of Technology.
- Yang, I. H., Joh, C., & Kim, B.-S. (2010). Structural behavior of ultra high performance concrete beams subjected to bending. *Engineering Structures*, 32(11), 3478–3487.
- Yoo, D. Y., Banthia, N., & Yoon, Y. S. (2016b). Flexural behavior of ultra-high-performance fiber-reinforced concrete beams reinforced with GFRP and steel rebars. *Engineering Structures*, 111, 246–262.
- Yoo, D. Y., Banthia, N., & Yoon, Y. S. (2017). Experimental and numerical study on flexural behavior of ultra-high-performance fiber-reinforced concrete beams with low reinforcement ratios. *Canadian Journal of Civil Engineering*, 44(1), 18–28.
- Yoo, D. Y., Kang, S. T., & Yoon, Y. S. (2016a). Enhancing the flexural performance of ultra-high-performance concrete using long steel fibers. *Composite Structures*, 147, 220–230.
- Zhou, J. L., Li, C., Yoo, D. Y., et al. (2022). Modified softened membrane model for ultra-high-performance fiber-reinforced concrete solid and hollow beams under pure torsion. *Engineering Structures*, 270, 114865.
- Zhu, Y. P., Zhang, Y., Hussein, H. H., et al. (2020). Flexural strengthening of reinforced concrete beams or slabs using ultra-high performance concrete (UHPC): a state of the art review. *Engineering Structures*, 205, 110035.
- Zhu, Y. P., Zhang, Y., Hussein, H. H., et al. (2022). Normal concrete and ultra-high-performance concrete shrinkage and creep models: development and application. *Advances in Structural Engineering*, 25(11), 2400–2412.

Publisher's Note

Springer Nature remains neutral with regard to jurisdictional claims in published maps and institutional affiliations.

Yanping Zhu Post-doc fellow at Missouri University of Science and Technology, Civil, Architectural and Environmental Engineering, Missouri 65401, USA.

Yang Zhang Professor at College of Civil Engineering, Hunan University, Changsha 410082, Hunan, China.

Xinze Yuan PhD at Missouri University of Science and Technology, Civil, Architectural and Environmental Engineering, Missouri 65401, USA.

Changgui Hou Graduate student at College of Civil Engineering, Hunan University, Changsha 410082, Hunan, China.